Transactions of the Materials Research Society of Japan 32[1] 87-90 (2007)

Compositional Dependence of the Piezoelectric Properties in $Pb(Zr_xTi_{1-x})O_3$ Thick films Prepared by a Chemical Solution Deposition Process

S. Osone, K. Brinkman, Y. Shimojo, and T.Ijima
Advanced Industrial Science and Technology, 1-1-1 Higashi, Tsukuba, Ibaraki, 305-8568
Fax: 81-29-8614845, e-mail: s.oosone@aist.go.jp

To investigate the compositional dependence of the piezoelectric properties in lead zirconate titanate (PZT) thick films, 2-μm-thickness $Pb(Zr_xTi_{1-x})O_3$ (x=0.2, 0.3, 0.4, 0.5, 0.6, 0.7, 0.8) films were prepared on $Pt/Ti/SiO_2/Si$ substrates by a chemical solution deposition process. The prepared thick films were fabricated into disk shape structure using reactive ion etching with a diameter of 10 μm and 20 μm. The ferroelectric properties and longitudinal displacement of the PZT thick film disks were measured simultaneously with an atomic force microscope (AFM) connected with a ferroelectric test system (FCE). Piezoelectric constants, referred to as *AFM* d_{33}, were calculated from unipolar driven strain-field curves. For ferroelectric properties, the coercive field *Ec* increased with decreasing Zr content, x, and remnant polarization *Pr* showed a peak at x= 0.4. On the other hand, the *AFM* d_{33} showed two peaks at x= 0.5 and 0.7. These tendencies are consistent with a simulation result for PZT ceramics (Yamamoto 1998 [1]). We suggest that the *AFM* d_{33} peak at x= 0.7 corresponds to the rhombohedral phase boundary between the high temperature, Rh (HT), and low temperature, Rh (LT) phases.
Key words: thick films, PZT, piezoelectric constant, chemical solution deposition

1. INTRODUCTION

Piezoelectric devices are used as actuators and ultrasonic devices. Lead zirconate titanate (PZT) is a representative material for piezoelectric devices because PZT has a high Curie temperature and a morphotropic phase boundary (MPB) displaying high values of the piezoelectric constant *d33*=233 pm/V. Yamamoto performed a simulation of the compositional dependence of the dielectric constant and the piezoelectric constant for $Pb(Zr_xTi_{1-x})O_3$ ceramics using a phenomenological thermodynamics approach and found that the piezoelectric constant has a peak at x= 0.5 and x= 0.7 at room temperature [1]. X= 0.5 corresponds to the MPB, and x= 0.7 corresponds to a phase boundary between a high temperature Rh (HT) and a low temperature Rh (LT)-Rhombohedral phase. Compositional dependence of the piezoelectric properties for $Pb(Zr_xTi_{1-x})O_3$ ceramics were measured and a peak at x= 0.5 and a low slope at x= 0.7 were confirmed [2].

The piezoelectric constant of thin films of several hundreds nanometer thickness was estimated as low as 50 pm/V [3, 4], values are relatively low compared with PZT ceramics. Therefore, there is increased interest in fabricating thick PZT films which have comparable piezoelectric property with the bulk PZT, but need lower applied voltages than ceramics. There are some studies of the compositional dependence of piezoelectric properties for thick films. Chen et al. measured the piezoelectric constant d_{33} for films with a thickness of 1μm and found a peak of d_{33} at the MPB [5]. Lederman et al. measured e_{31} for films with thickness of 4μm and found a peak of e_{31} at MPB [6]. Although it is believed that thick films have similar properties as the bulk PZT, a peak at x= 0.7 has not been observed in films.

Here, a compositional dependence of piezoelectric property was measured for films with a thickness 2μm. The measurement condition is important, as actual d_{33} value can not be measured with a large diameter of an electrode for films. The PZT film is constrained by the Si substrate, and a clamped condition exists. With a larger diameter of an electrode, the Si substrate and PZT films bend toward the top electrode when a field is applied and the strain becomes smaller. Li et al. did a finite element method (FEM) simulation concerning an aspect ratio D/t (D is a diameter of an electrode, t is a thickness of films) for PZT thin films and found the best condition as D/t~1 [7]. Okino et al. (2006) did a FEM simulation and showed an etched PZT (not a continuous PZT) as the best condition for a double beam interferometry and an atomic force microscopy (AFM) [8]. We have found an experimental result of best condition D/t <3 for films with a thickness 10μm of an etched PZT [9]. The preparation of D/t ~1 is difficult because of the small sizes needed in fabrication. Therefore, an aspect ratio as small as possible, D/t=5 was prepared with a diameter of an electrode 10μm for a 2μm thickness film of etched PZT. The relative d_{33} can be compared among PZT films which have same aspect ratio D/t. Larger aspect ratio, D/t=10 was so prepared with a diameter of an electrode 20μm in order to confirm the clamping effect

2. EXPERIMENTAL PROCEDURE

To prepare the chemical solution precursor of $PbTiO_3$ and $PbZrO_3$, we used trihydrated lead acetate (99.9%, Nacalai tesque), titanium isopropoxide (99.999%, Aldrich) and zirconium n-propoxide (70% in proponol, Azmax), and 2-methoxyethanol as the solvent. The concentration of the solution was controlled to 0.5M. Before the film deposition process, various volumes of $PbTiO_3$ and $PbZrO_3$ precursor solution were mixed to control the final composition like $Pb(Zr_xTi_{1-x})O_3$, x =

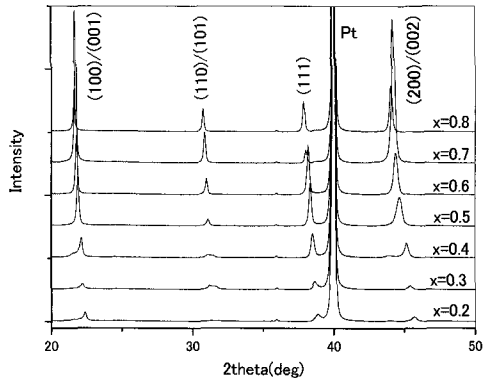

Fig1.X-ray diffraction spectrum for $Pb(Zr_xTi_{1-x})O_3$.

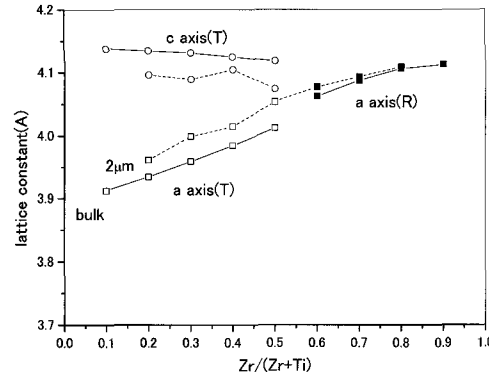

Fig.2 Composition dependence of lattice constant. The lattice constant of bulk is referred [10].

0.2- 0.8 by step 0.1 that corresponds to Zr content. After the mixing process, the solution was stable. Seven kinds of mixed solution were deposited onto $Pt/Ti/SiO_2/Si$ substrate using a spin coater operated at 3000 rpm. The sequence of the process, comprising a spin coating, drying at 120°C for 1min, a pyrolysis at 400°C for 3 min and anneal at 700°C for 3min in pure oxygen were performed several times to control the film thickness. Pt top electrodes were deposited onto the films using a sputtering method. The Pt top layer and PZT layer were dry etched using a reactive ion etching to create disks with a diameter 10μm and 20μm.

The X-ray diffraction spectrum was measured with a Philips X'pert. AFM probing system was connected with a ferroelectric test system FCE to measure a polarization- field (*P-E*) hysteresis curves and a longitudinal displacement-field curves simultaneously with an AFM conductive cantilever. The cantilever was touched on the top electrode in a contact mode, and a bipolar and a unipolar drive voltages with 5Hz were applied to the sample. The longitudinal displacement was estimated with a Z height signal of the AFM

3. RESULTS AND DISCUSSION

3.1 Crystal structure

For the X-ray diffraction analysis, all patterns show a well defined perovskite structure in addition to Pt (111) as shown in fig.1. As a Zr content x decreases, 2 theta angle of the peak shift to larger. A clear difference of (100) and (001) and that of (200) and (002) were observed at a tetragonal phase x= 0.4- 0.2. Each peak was fitted with a Gaussian and a second order linear function and a diffraction angle of a peak was obtained. The diffraction angle of PZT was calibrated so that a diffraction angle of Pt for all composition was the same. The lattice constant was calculated from the (100) peak and the (111) peak for x= 0.2- 0.5 using a tetragonal equation and from the (200) peak for x= 0.5- 0.8 using a rhombohedral equation. The compositional dependence of a lattice constant is shown in fig.2. With increasing Zr content x, a lattice constant of *c*- axis is decreased and that of *a*- axis is increased. With x= 0.5, the value of *a*- axis and *c*- axis is almost same. The lattice constant of *a*- axis is increased with a increase of a Zr content x in the rhombohedral phase. It is confirmed that the MPB from a tetragonal to a rhombohedral is around x= 0.5. This result is consistent with PZT ceramics and PZT thin films.

3.2 ferroelectric properties

The spot of a diameter of an electrode 20μm is used for *P-E* hysteresis curve for x= 0.3, 0.5, 0.7 at an electric field 167 kV/cm are shown in fig.3 The coercive field increased with an decrease of Zr content x. The remnant polarization is largest at x= 0.5. The unipolar voltage is applied with a step of 5V and a remnant polarization was measured. The field dependence of a remnant polarization for each composition is shown in fig.4.

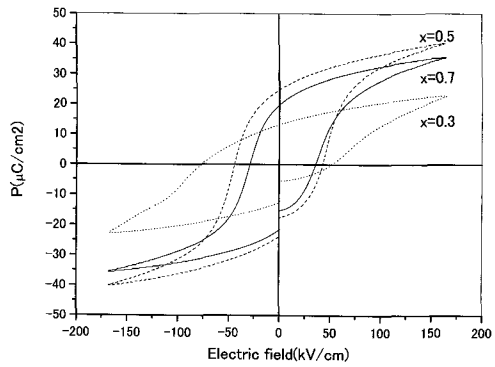

Fig.3 The *P-E* hysterics for 20μm diameter of electrode.

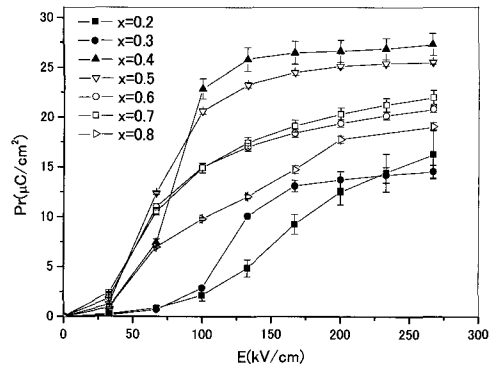

Fig.4 Field dependence of remnant polarization for 20μm diameter of electrode.

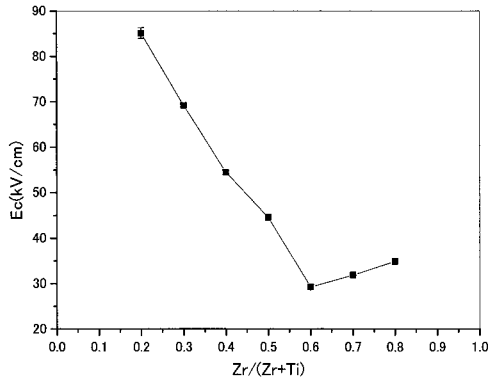

Fig.5 The compositional dependence of the coercive field for 20μm diameter of an electrode.

The error of the physical value is given from measurement of different spots. The remnant polarization for all composition saturates at an electric field 167 kV/cm. Therefore, a remnant polarization and a coercive field for all compositions are compared with an electric field 167 kV/cm. The composition dependence of a coercive field and a remnant polarization is shown in fig.5 and fig.6. The coercive field increased with a decrease of a Zr content x. The remnant polarization has a maximum at x= 0.4. These tendencies are consistent with an experimental result of Chen et al. [5].

3.3 Piezoelectric Property

The longitudinal displacement curves for x= 0.2, 0.5, 0.8 with 10μm diameter electrode is shown in fig.7. When strain is compared with same electric field, strain is largest at x= 0.5. Unipolar driven longitudinal strain under a coercive field for x= 0.5 is shown in fig. 8. The strain increased linearly and was in proportion to the applied field. The longitudinal piezoelectric constant defined as *AFM* d_{33} was calculated from the field-strain line slope as shown in fig.8. The compositional dependence of *AFM* d_{33} for two kinds of a diameter of an electrode is shown in fig.9. The error of physical value is calculated from a measurement of different spots. The maximum peak of *AFM* d_{33} is obtained at x= 0.5 and second peak is obtained at x= 0.7. This tendency is obtained for two kinds of a diameter of an electrode.

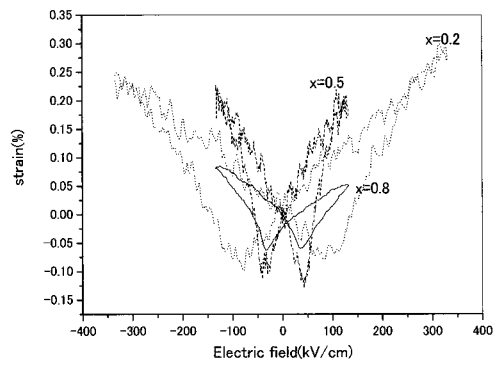

Fig.7 The longitudinal displacement curve with 10μm diameter electrode.

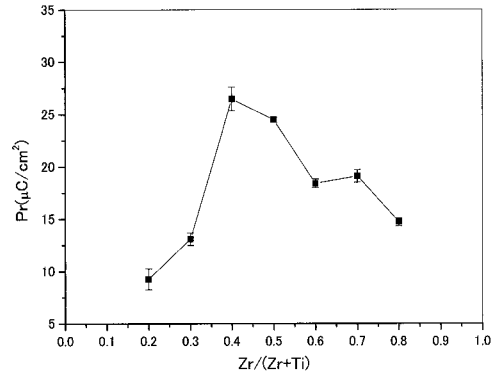

Fig.6 The compositional dependence of the remnant polarization for 20μm diameter of an electrode.

These tendencies are consistent with a simulation result [5] and an experimental result [6] for ceramics.

There is a difference between *AFM* d_{33} for an aspect ratio D/t =5 of 10μm diameter of an electrode and that for D/t =10 of 20μm diameter of an electrode. *AFM* d_{33} is smaller for a larger D/t. This is due to a clamping effect. This is consistent with a simulation result of Li et al. [7].

Moreover, the effect of a poling on an unipolar driven longitudinal strain was investigated for a diameter of an electrode 10μm. The dc voltage which was three or four times as high as coercive field, was applied at room temperature. After applying the voltage for 5min, the unipolar driven longitudinal strain under a coercive field was measured to calculate the *AFM* d_{33}. The compositional dependence of the *AFM* d_{33} with a poling and without poling are compared in fig. 10. The *AFM* d_{33} increased slightly with a poling. The maximum peak of the *AFM* d_{33} is obtained at x= 0.5 and a second peak of that is obtained at x= 0.7 after a poling.

4. CONCLUSION

$Pb(Zr_xTi_{1-x})O_3$ (x= 0.2, 0.3, 0.4, 0.5, 0.6, 0.7, 0.8) films with a thickness of 2μm were prepared. Two different diameter of an electrode 10μm, 20μm were prepared as an etched PZT. The coercive field decreases with a Zr content x and the remnant polarization has a peak at x= 0.4. These tendencies were almost consistent with a observation result of Chen et al. [5]. The maximum peak

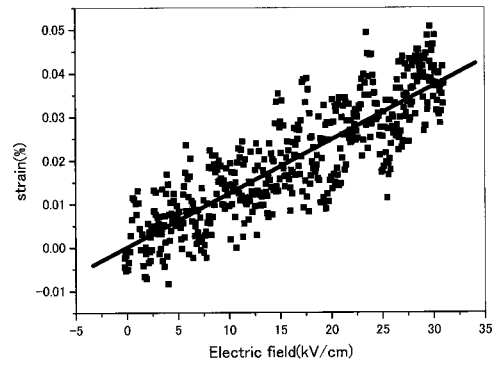

Fig.8 The unipolar driven longitudinal strain for x= 0.5.

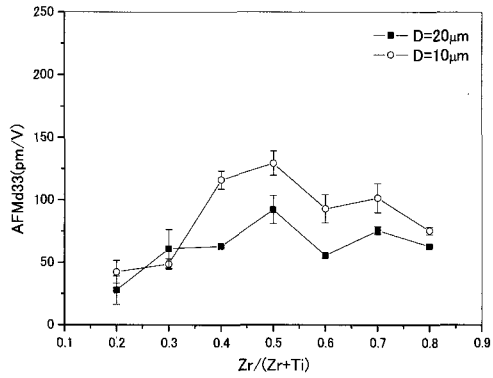

Fig. 9 The compositional dependence of *AFM* d_{33} for two kinds of an electrode.

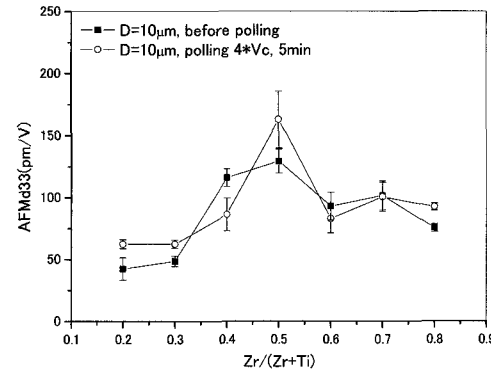

Fig.10 The comparison of *AFM* d_{33} without a polling and with a polling for 10μm diameter of an electrode.

of *AFM* d_{33} is obtained at x= 0.5 and a second peak is obtained at x= 0.7. Moreover, an effect of a poling on *AFM* d_{33} was investigated for 10μm diameter of an electrode. The maximum peak of *AFM* d_{33} is obtained at x= 0.5 and second peak is obtained at x= 0.7 after a poling. This tendency is consistent with a simulation result of PZT ceramics [1]. X= 0.7 corresponds to a rhombohedral phase boundary between a high temperature and a low temperature phase.

5.REFERENCES

[1]T. Yamamoto, Jpn. J. Appl. Phys., 37, 1998, 6041.
[2]H. Ouchi, K. Nagano and S. Hayakawa, J.Ame.Ceram. Soc., 1965, 48, 630.
[3]D.J. Kim, J.P. Maria, A.I. Kingon, and S.K. Streiffer, J. Appl. Phys., 93, 2003, 5568.
[4]S. Hiboux, P.Muralt, and T.Maeder, J. Mater. Res., 14, 1999, 4307
[5]H.D. Chen, K.R. Udayakumar, C.J. gaskey, and L.E. Cross, Appl. Phys. Lett., 67, 1995, 3441.
[6]N. Lederman, P. Muralt, J. Baborowski, S, Gentil, K. Mukati, M. Cantoni, A. Seifert, and N. Setter, Sensors and Actuators A, 105, 2003, 162.
[7]J.H. Li, L. Chen, V.Nagarajan, R. Ramesh, and A.L. Roytburd, Appl. Phys. Lett. 84, 2004, 2626.
[8]H.Okino, M. Hayashi, T.Iijima, S.Yokoyama, H. Funakubo, N.Setter, and T.Yamamoto, MRS, 902E-T03-49.1, 2006.
[9]T. Iijima, S.Osone, Y. Shimojo, H. Okino, and T. Yamamoto., MRS, 902E-T03-09.1, 2006
[10] Landolt-Bornstein, vol.16, 427

(Received December 28, 2006;Accepted January 5, 2007)